Surface & Coatings Technology 352 (2018) 411–419

Contents lists available at ScienceDirect

Surface & Coatings Technology

journal homepage: www.elsevier.com/locate/surfcoat

Preparation and tribological properties of graphene oxide doped alumina composite coatings

Hongfei Yin[a], Qingwen Dai[a], Xiaodong Hao[b], Wei Huang[a,*], Xiaolei Wang[a]

[a] College of Mechanical & Electrical Engineering, Nanjing University of Aeronautics & Astronautics, Nanjing 210016, China
[b] Automation Research & Design Institute of Metallurgical Industry, Beijing 100071, China

ARTICLE INFO

Keywords:
Graphene oxide
Al_2O_3
Coating
Electro-deposition
Wear resistance

ABSTRACT

In this paper, nickel matrix composite coatings incorporated with graphene oxide (GO) and graphene oxide doped alumina (GO-Al_2O_3) particles were fabricated through electro-deposition. Given the excellent mechanical properties of GO and Al_2O_3, excellent anti-wear properties are expected when embedding GO-Al_2O_3 particles in Ni matrix. For this purpose, nano-Al_2O_3 particles were first grafted on GO surfaces to fabricate the GO-Al_2O_3 particles. The structure, composition and morphology of the GO and GO-Al_2O_3 were characterized by XRD, FT-IR, SEM, TEM and BSE, respectively. The results revealed that nano-Al_2O_3 particles were successfully doped on GO surfaces. The tribological performances of the coatings were studied under dry sliding condition. It was found that the wear rate of Ni/GO composite coating declined by 20.9% compared to pure Ni coating. The results also indicated that the Ni/GO-Al_2O_3 coatings with higher amount of Al_2O_3 content presented the lower friction coefficients and better anti-wear behaviors. The superior tribological properties of the Ni/GO-Al_2O_3 coating were attributed to the synergistic effects of GO and Al_2O_3.

1. Introduction

Failure of most engineering components occurs at the surface, corrosion begins from the surface, fatigue cracks propagate inwards from the surface and wear also occurs on the surface [1]. Surface coating is a typical method of surface engineer, and it plays an important role to improve the service performance of components.

Composite electroplating, as a coating technology, is a method by which fine particles are co-deposited with a metal or alloy matrix [2]. During the fabrication process, insoluble particles are suspended in a conventional plating electrolyte and captured into the growing metal coatings. The micro-hardness, yield strength tensile strength [3], anti-corrosion [4,5] and oxidation [6] of the coatings are improved by the presence of the second-phase particles. Wear resistance is another important application for the co-deposition coatings. The traditional dispersed phase can be hard oxide (SiO_2 and Al_2O_3), carbides (SiC and WC), diamond or polymer (PTE and PTFE) [7–9]. The incorporation of hard particles act as a load-bearing element [10] and the polymers usually work as lubrication phase [8].

Recently, graphene has attracted tremendous interests in tribological area [11–13]. However, it contains rare surface functional groups with limited dispersibility in solvents [14]. The hydrophilic graphene oxide (GO) is an oxygenated derivative of graphene and it can be easily dispersed in polar solvents, which made it a facile material to fabricate composite coatings by the electrochemical technology [15]. Similar to graphene with the layer structure, GO is expected as a good solid self-lubricant. The composite coatings, co-depositing GO as a second-phase, exhibit excellent tribological performances. Liu et al. [16] found that the incorporating GO greatly improves the friction reduction and wear resistance of the Co/GO composite coating. Algul et al. [17] reported that the increment of GO content in the Ni/GO coatings result in significant increase in the micro-hardness and the wear resistance, as well as a decrease in friction. Xue et al. [18] introduced Ni/GO composite coatings produced by electro-deposition under supercritical carbon dioxide. This Ni/GO film presents lower surface roughness and smaller grain size. Meanwhile, the incorporations of GO in the coating improve the wear resistance and friction reduction. The tribological performances of electroless Ni−P coatings are improved when embedding GO [19] and the subsequent research found that appropriate heat treatment can also enhance the micro-hardness as well as wear resistance of Ni-P-GO coatings [20]. Usually, the wear rate of the composite coatings decreases with the enhancing of GO content.

In this paper, combined with the excellent lubricity of GO and load bearing capacity of hard particle, attempt has been made to develop GO doped nano-Al_2O_3 powder (GO-Al_2O_3) as co-depositing particles. The properties of the GO and GO-Al_2O_3 were characterized. Composite

* Corresponding author at: Yudao street 29#, Nanjing, China.
E-mail address: huangwei@nuaa.edu.cn (W. Huang).

https://doi.org/10.1016/j.surfcoat.2018.08.042
Received 2 October 2017; Received in revised form 11 August 2018; Accepted 13 August 2018
Available online 14 August 2018

coatings of Ni/GO and Ni/GO-Al_2O_3 were prepared via electro-deposition and the tribological performances of the coatings were evaluated. The effect of the ratio relation between the GO and Al_2O_3 hard particle in the composite coatings was also discussed.

2. Experimental section

2.1. Synthesis of GO and GO-Al_2O_3

GO was prepared from purified natural graphite by a modified Hummer's method that involves a strong oxidation of graphite powder with H_2SO_4/$KMnO_4$ and exfoliation process in solution. The specific procedure can be found in ref. [21, 22]. The GO-Al_2O_3 powder was obtained through a self-assembling process under the effects of electrostatic interaction. Briefly, 0.1 g of GO was dispersed in 50 mL deionized water. And 1.0 g of commercial Al_2O_3 powder with the size of about 50 nm was added to 100 ml acetic acid solution with the concentration of 0.5 mol/L and the pH value was about 3–4. The solutions were both dispersed using ultrasonic treatment for 1 h. Subsequently, the GO suspension was slowly added to the Al_2O_3 under continuous stirring. Then, the mixture was moved to oil bath and heated to 120 °C for 24 h. After that, the suspension was filtered and washed with purified water to remove by-products. The dried GO-Al_2O_3 powder was ground by ball-milling in vacuum for 12 h at the speed of 80 rpm. During the experiment, the ratio of GO: Al_2O_3 was reached by changing the mass ratio of GO and Al_2O_3 in the suspension. Produced GO-Al_2O_3 composites in this paper are characterized with the following mass ratio (GO: Al_2O_3) of 1:1, 1:2, 1:5 and 1:10, respectively.

2.2. Electro-deposition

Nickel (Ni), composite (Ni/GO) and (Ni/GO-Al_2O_3) coatings were fabricated using the electro-deposition method. The volume of the deposition bath is about 500 mL and the distance between anode and cathode is controlled at 5 mm. And the pure Ni plate is used as anode. The composition of Watts bath and specific experimental conditions are shown in Table 1. Prior to the deposition, GO and GO-Al_2O_3 powders respectively, were ultrasonically dispersed in the plating bathes for 15 min. A copper plate with Φ30 × 3 mm was used as the substrate and its surface was mechanically polished to Ra 0.1–0.15 μm. The substrate was then activated for 20 s in a mixed acidic bath followed by ultrasonic cleaning with acetone and deionized water for 5 min, respectively. All electroplating times were fixed at 120 min. After that, the final coatings were ultrasonically cleaned in acetone and washed with running water.

2.3. Characterizations

The structures of the GO and GO-Al_2O_3 powders were detected via X-ray diffraction using an X'Pert Pro diffractometer (Panalytical) at a scan rate of 2°/min. Fourier transform infrared (FT-IR) spectra of the samples dispersed in KBr pellets was recorded on an infrared spectroscopy (NEXUS870, NICOLET). The morphology of the powder samples were determined using a transmission electron microscope (TEM, JEOL JEM-200CX) and a scanning electron microscopy (SEM, Hitachi S3400). EDS and BSE were used to further confirm the component and distribution of GO-Al_2O_3 powder.

The cross-sectional microstructures and surface morphology of the coatings were observed by a scanning electron microscopy (SEM, JSM-6480LV) and the EDS analysis was performed to detect the element content. The elementally X-ray maps from the cross-section of Ni/GO-Al_2O_3 composite coating were detected using an energy dispersive X-ray spectrometer. The micro-hardness of the coating surfaces was determined using a Vicker's microhardness indenter with a load of 100 g for 10 s. At least ten points along the radius direction were tested and the final hardness was an average of the ten points.

Ball-on-disc tests were performed to determine the anti-wear properties of the coatings under dry condition. A standard 304 stainless steel ball with a diameter of 4.0 mm was used as the upper specimen. All tests were carried out under a 2 N load with a sliding speed of 0.1 m/s. The wear topography of the coatings was observed by SEM. The volumetric loss of the coatings after friction test was measured using a surface profilometer (Bruker, ContourGT-K) and the wear rates were calculated based on the volumetric loss.

Table 1
Experimental condition for the electro-depositions.

Compositions and conditions	
Nickel sulfate, $NiSO_4·6H_2O$ (g/L)	300.0
Nickel chloride, $NiCl_2·6H_2O$ (g/L)	45.0
Boric acid, H_3BO_3 (g/L)	40.0
Sodium dodecyl sulfate (g/L)	0.5
Saccharin sodium (g/L)	1.0
Particle concentration (g/L)	0, 0.5
Temperature (°C)	45
pH	4 ± 0.5
Current density (A/dm^2)	2
Magnetic stirring speed (rpm)	200

3. Results and discussion

3.1. XRD analysis

Fig. 1 shows the XRD patterns of GO and GO-Al_2O_3 powders. The GO depicts a strong and broad diffraction peak at 2θ of 9.62° and a corresponding d-spacing of 0.91 nm, which is due to the presence of oxygen functionalities in the basal plane of natural graphite [23]. A mild and broad peak at around 20° suggests the thorough graphitic crystal structures. According to the XRD pattern of GO-Al_2O_3 powder, the crystalline structure of alumina is corundum and the peak at 10° belongs to GO. Apart from corundum and GO, no other phase was detected.

3.2. FT-IR analysis

Fig. 2 shows the FT-IR data of GO-Al_2O_3 composite powders, and the pure alumina powder without GO was also given for comparison. The spectrum of GO-Al_2O_3 shows the representative groups of Al_2O_3 and GO. The characteristic absorption of Al—O bond at 640 cm^{-1} was observed for both GO-Al_2O_3 and Al_2O_3 [24]. The presence of oxygen-containing functional groups at 1230 cm^{-1}, 1567 cm^{-1} and 1720 cm^{-1}

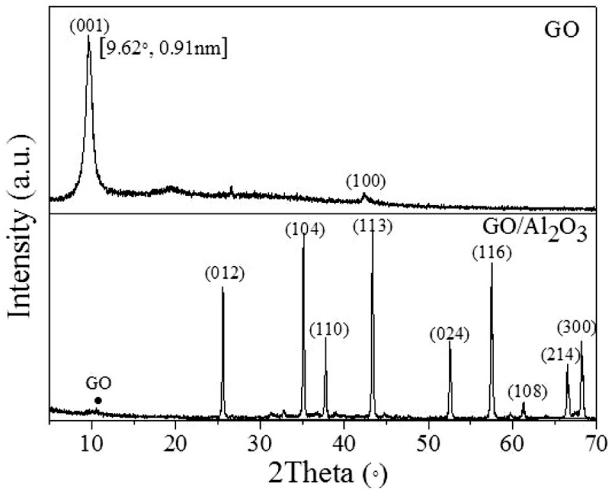

Fig. 1. X-ray diffraction (XRD) patterns of GO and GO-Al_2O_3 powders.

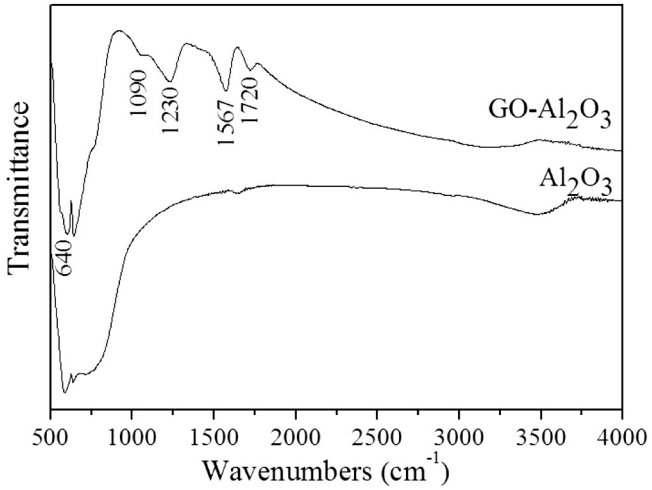

Fig. 2. FT-IR spectra of the GO-Al_2O_3 and Al_2O_3 powders.

are corresponding to C—OH stretching vibration, C=C stretching vibration, and C=O stretching vibration of COOH groups [25,26]. One characteristic peak of the composite powders is observed at around 1090 cm^{-1}, which corresponds to Al—O—C bonding [27]. And this bonding implies that GO-Al_2O_3 powder induces the formation of chemical bonding between GO and Al_2O_3.

3.3. Morphology analysis

Fig. 3 shows the morphologies of GO and GO-Al_2O_3. In Fig. 3a, the lamellar structure with wrinkled film morphology is observed for GO sample. In addition, GO sheets aggregate and demonstrate a stacking state, which can be attributed to their high specific area. Different degrees of transparency of GO can be seen in Fig. 3c and some dark lines with large contrast can also be found, which clearly illustrates that GO sheets are wrinkled or folded. The electron diffraction pattern reveals that the GO sheets are hexagonal close-packed crystal structure with several layers. The SEM image of GO-Al_2O_3 shows that the Al_2O_3 nanoparticles are supported on the layered structure of GO (see Fig. 3b) and the TEM image of GO-Al_2O_3 manifests that Al_2O_3 particles are

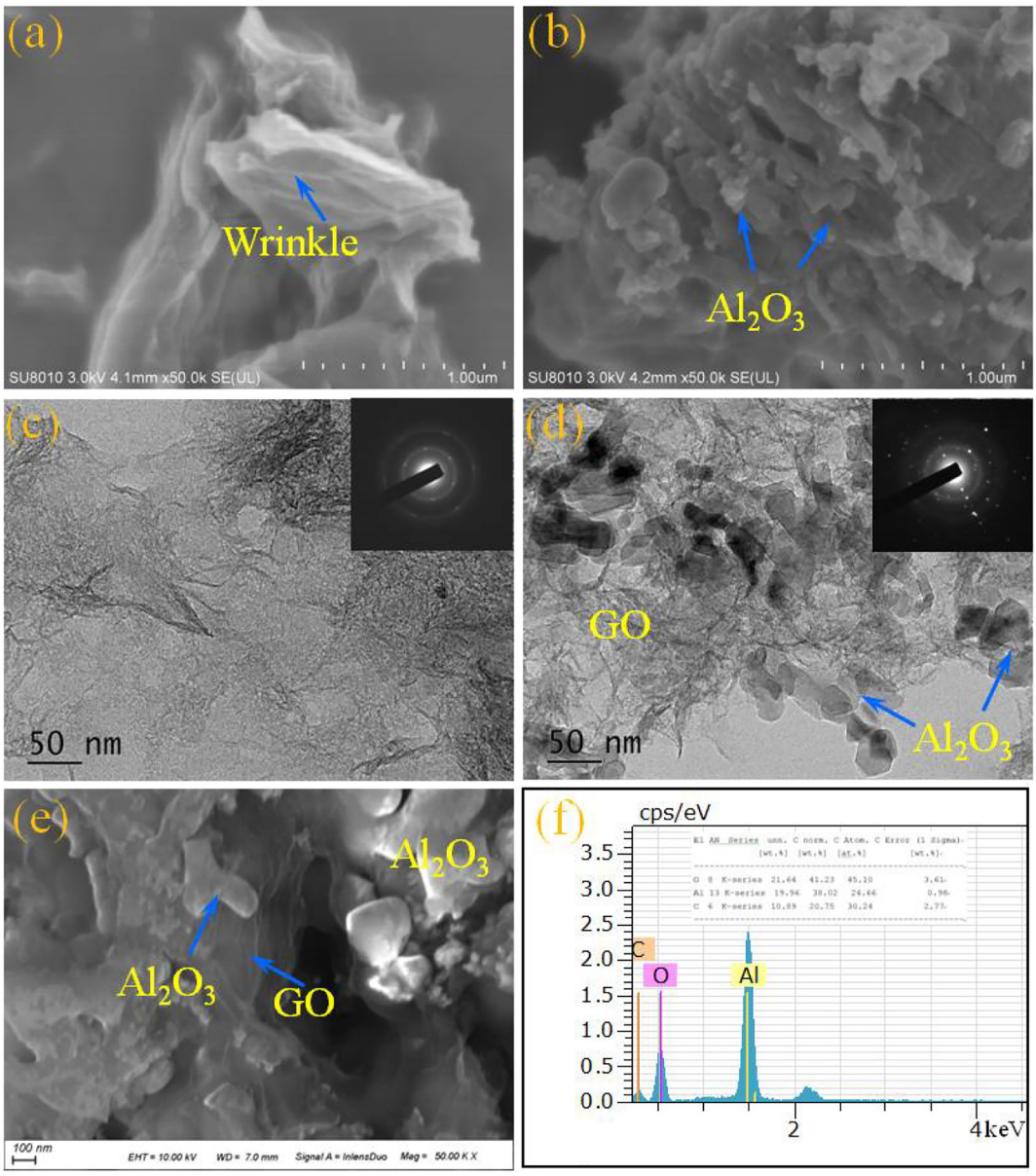

Fig. 3. SEM images of (a) GO and (b) GO-Al_2O_3; TEM images of (c) GO and (d) GO-Al_2O_3; (e) BSE of GO-Al_2O_3; (f) EDS of GO-Al_2O_3.

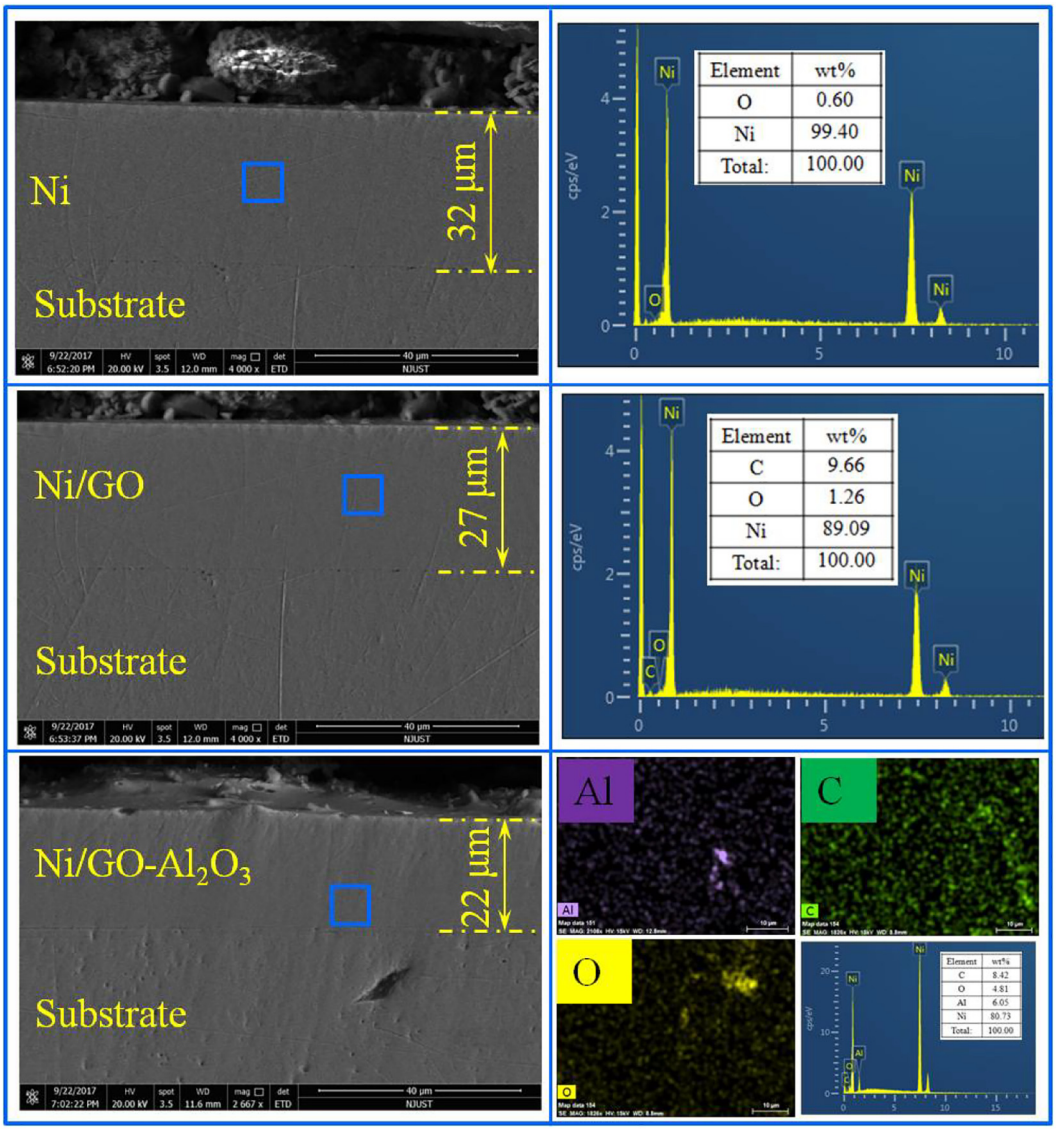

Fig. 4. Cross-sectional morphologies and corresponding EDS of the three coatings, Elementally X-ray maps for Al, C and O in Ni/CO-Al_2O_3 coating was given. The mass ratio (GO: Al_2O_3) for Ni/GO-Al_2O_3 coating is 1:1.

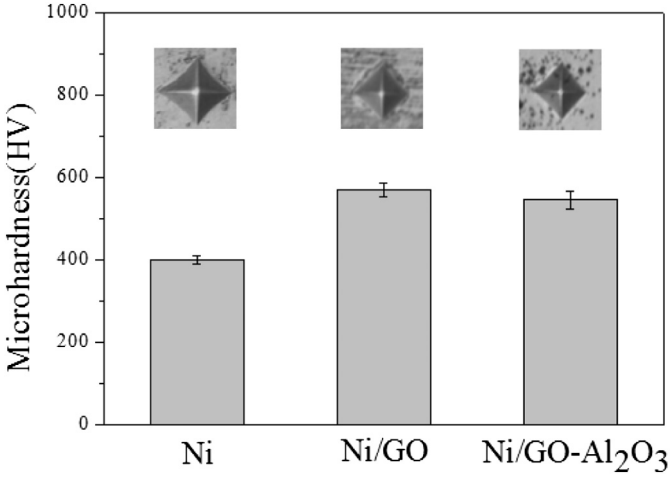

Fig. 5. Microhardness of the three coatings, the mass ratio (GO: Al_2O_3) for Ni/GO-Al_2O_3 coating is 1:1.

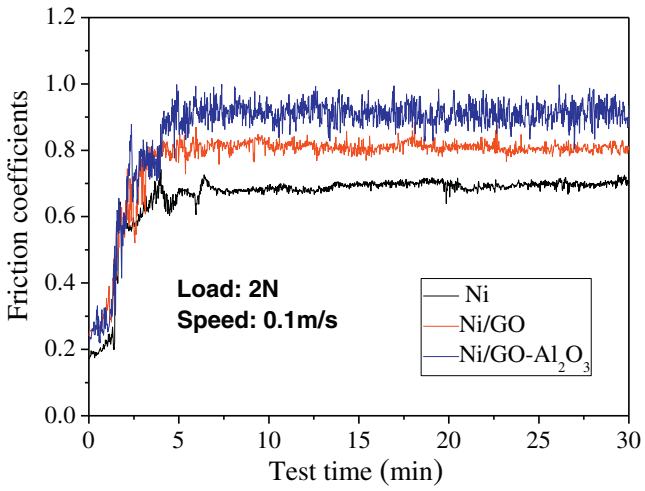

Fig. 6. The friction curves of the three coatings under dry sliding conditions, the mass ratio (GO: Al_2O_3) for Ni/GO-Al_2O_3 coating is 1:1.

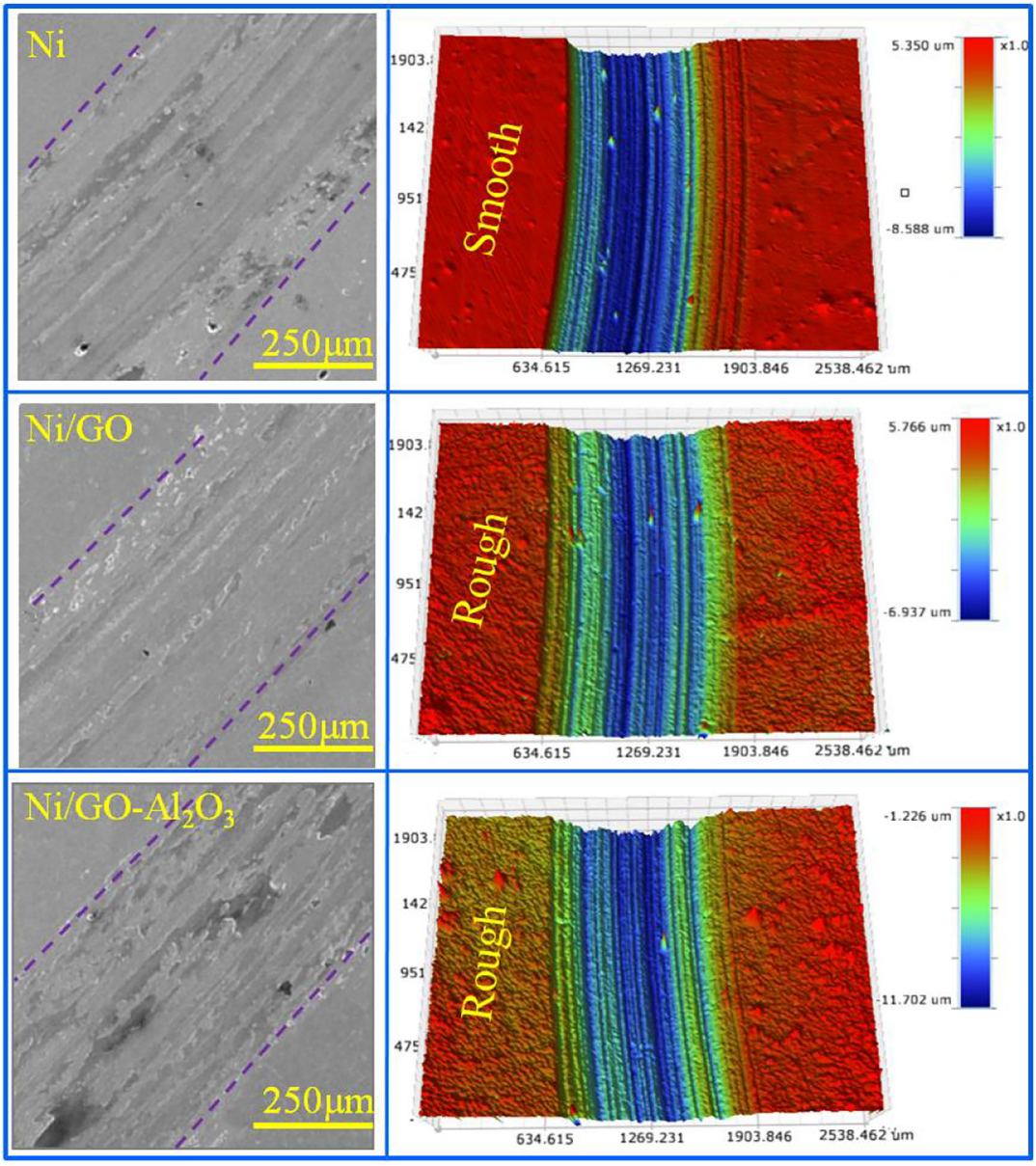

Fig. 7. Microscopic and 3D images of the worn tracks under dry sliding conditions, the mass ratio (GO: Al_2O_3) for Ni/GO-Al_2O_3 coating is 1:1.

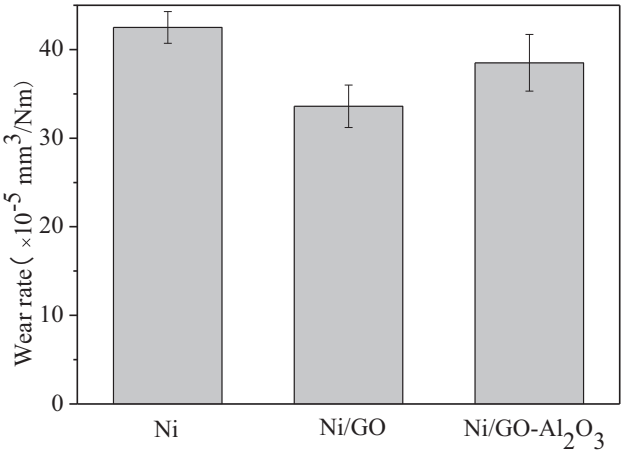

Fig. 8. Wear rates of the three coatings under dry sliding conditions, the mass ratio (GO: Al_2O_3) for Ni/GO-Al_2O_3 coating is 1:1.

assembled on the thin surface of GO. Similar to Fig. 3c, severe agglomeration among GO occurred. Al_2O_3 particles in GO-Al_2O_3 can be distinguished by BSE image (see Fig. 3e) and the EDS spectrum of GO-Al_2O_3 shows the presence of C, O and Al elements (see Fig. 3f).

3.4. Cross-sectional morphologies and hardness of the coatings

Representative SEM micrographs of the cross-sectional profiles of the pure Ni, Ni/GO and Ni/GO-Al_2O_3 coatings are depicted in Fig. 4. In general, the coatings are well bonded to the substrate without obvious defects and impurities visible at the interface. Since different part of the coating may have different thicknesses, the thickness was measured along the diameter direction for each sample and at least ten measurements were conducted. The final value was averaged from the ten points. For the same plating conditions, the Ni coating with the largest average thickness of 32 ± 2 μm was observed, compared with Ni/GO (27 ± 1.5 μm) and Ni/GO-Al_2O_3 (22 ± 1.5 μm) coatings. The decreased deposition rate for the composite coatings may be caused by the changing of the current efficiency. Based on the weight increment, the

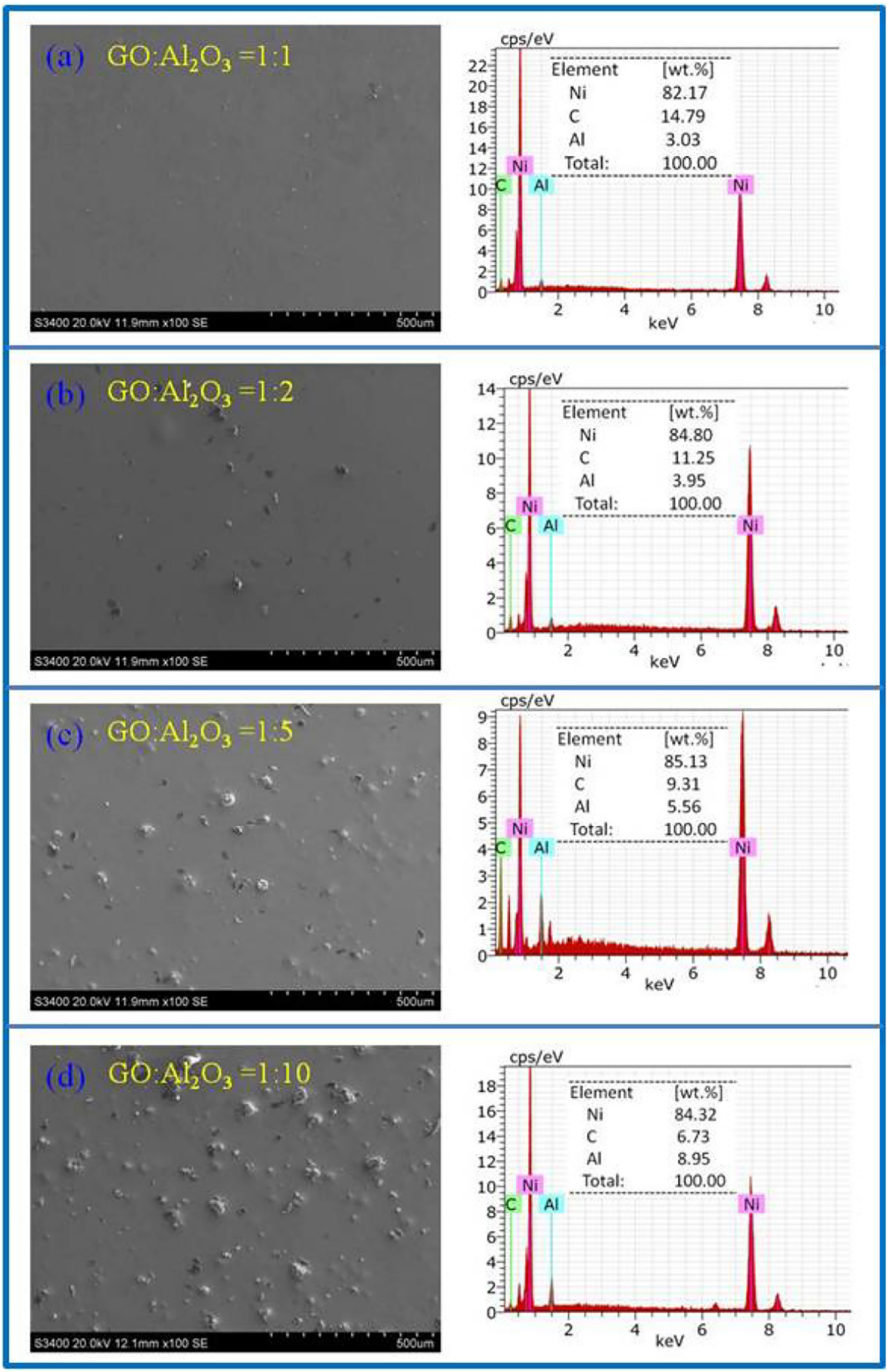

Fig. 9. SEM images of Ni/GO-Al_2O_3 composite coatings and corresponding EDS spectrums with different GO:Al_2O_3 mass ratios.

current efficiency of the coatings was calculated and the values were 85.3% (Ni), 78.2% (Ni/GO) and 69.3% (Ni/GO-Al_2O_3), respectively. With the incorporation of the particles in the coatings, cathode current density increases, leading to the aggravating evolution of hydrogen. That's the reason why the current efficiency decreases for the composite coatings. Due to the insulation characteristic of Al_2O_3, Ni/GO-Al_2O_3 coating shows the lowest current efficiency as well as the deposition rate. As can be seen in Fig. 4, the element of C with the content of

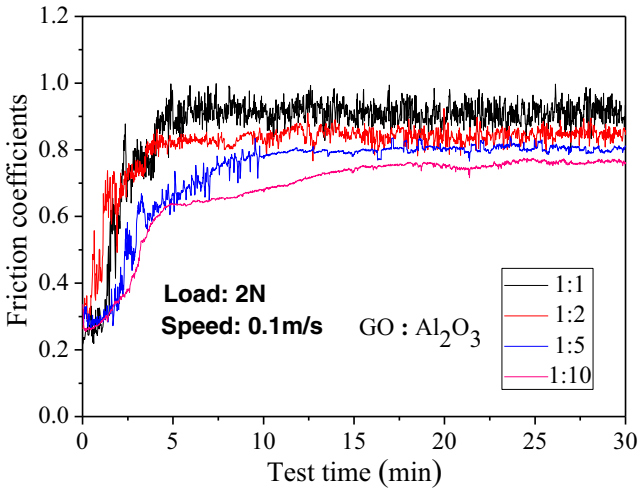

Fig. 10. The friction curves of Ni/GO-Al_2O_3 coatings with different mass ratio of GO and Al_2O_3.

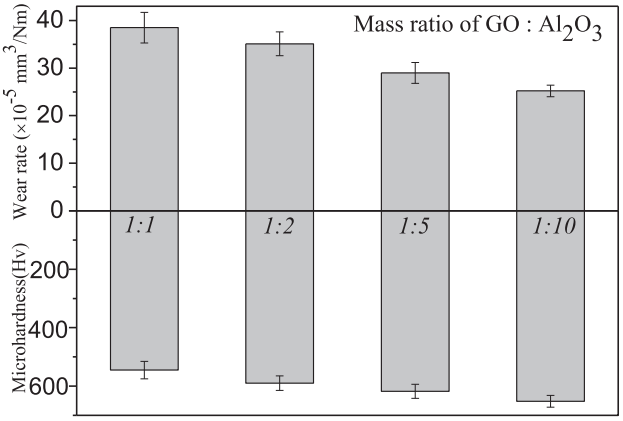

Fig. 11. Wear rates and micro-hardness of Ni/GO-Al_2O_3 coatings with different mass ratio of GO and Al_2O_3.

9.66 wt% was detected in Ni/GO coating according to the EDS analysis. The elementally X-ray maps show that elements of Al, C and O are uniformly distributed in the Ni/GO-Al_2O_3 composite coating.

Fig. 5 demonstrates the surface hardness of the three typically coatings. The mean value of hardness was calculated with over ten tests on the surfaces along the radius direction. As expected, the hardness increases by 35% when GO incorporated in Ni matrix, since GO sheets possess high strength and modulus [14]. As can be seen in Fig. 4, carbon content declines from 9.66 wt% in Ni/GO to 8.42 wt% in Ni/GO-Al_2O_3 coating. The slight decrease of hardness may be caused by the decrement of GO in Ni/CO-Al_2O_3 coating. In general, the hardness of composite coatings depends on the incorporation of particles, which can be attributed to the traditional dispersion-strengthening mechanism [28,29]. In addition, the particles in composite coating can also act as a barrier to plastic deformation of Ni matrix [30].

3.5. Tribological performance of the coatings

Fig. 6 shows the friction curves of the three coatings under dry sliding condition. The friction coefficients are approximately 0.7–0.9, and the pure Ni exhibits the lowest coefficient among the three types of coatings. Different from the previous reports [15,26,31–34], self-lubricating effect of GO in Ni/GO coating does not appear, compared with pure Ni coating. As mentioned in ref. [13], the high modulus of graphene may hinder the formation of the lubricating film. In addition, the coefficient increment by the introduction of GO in the epoxy matrix was also reported by Shen et al. [35], and the wrinkled surface morphology of GO was the main reason, which would roughen the surface of the composites. Similar friction coefficient (0.8) of Ni/GO coating was also reported in ref. [18] and the increased coefficient was attributed to the high surface roughness. In reality, it was observed that the composite coatings show the rougher surfaces compared to pure Ni coating as can be seen in Fig. 7 (3D images).

Although the friction coefficient of Ni/GO coating is a litter higher than that of pure Ni coating, it exhibits obvious anti-wear performance. Fig. 7 depicts the microscopic and corresponding three-dimensional images of the worn tracks. Compared with composite coatings, the track on Ni coating shows deep scratches and grooves, indicating severe plastic deformation. While in the present of GO and GO-Al_2O_3, the widths of wear tracks decrease slightly and present the shallower and smoother features. As shown in Fig. 8, Ni/GO composite coating exhibits obviously wear resistance and the wear rate reduces by 20.9% compared to pure Ni coating. The decrease of wear rate for the Ni/GO composite coating can be explained as follow: First, the wear rate is inversely proportional to the hardness of material according to the classical Archard's law. And the inclusions of GO enhance the hardness of the composite coating, leading to the improved wear resistance. Second, the excellent ductility of GO sheets can release the residual stress from wear via the micro plastic deformation or migration [36]. In Figs. 7 and 8, it is also found that the frictional and anti-wear performances of Ni/GO coating are both superior to Ni/GO-Al_2O_3 when the mass ratio of GO: Al_2O_3 is 1:1.

A question then arises: compared with Ni/GO coating, can better tribological behaviors be achieved when introducing Al_2O_3? To answer this question, Ni/GO-Al_2O_3 coatings were prepared using GO doped Al_2O_3 powders with different mass ratios.

Fig. 9 presents the surface morphologies and corresponding EDS spectrums of Ni/GO-Al_2O_3 composite coatings with different GO: Al_2O_3 mass ratios. The surface is smooth at the low mass ratio of Al_2O_3 (see in Fig. 9a) and the nodular structures were observed with the increase of Al_2O_3. The EDS analysis shows that element Al in the coatings increases with the increasing Al_2O_3 content in the electrolytes. When changing the mass ratio of GO: Al_2O_3 from 1:1 to 1:10, the amount of element Al embedded in the composite coating enhances from 3.03 wt% to 8.95 wt % and the element C decreases from 14.79 wt% to 6.73 wt%.

Friction curves of the four samples are shown in Fig. 10. Fig. 11 presents the corresponding wear rate and micro-hardness of Ni/GO-Al_2O_3 coatings. At the lower ratio of Al_2O_3 (GO:Al_2O_3 is 1:1 and 1:2), the friction coefficients and wear rates of Ni/GO-Al_2O_3 coatings are still higher than that of Ni/GO coating. And the anti-wear property of Ni/GO-Al_2O_3 coatings with less amount of Al_2O_3 is still inferior to Ni/GO.

While the ratio reaches 1:5, not only the coefficient, but the wear rate of Ni/GO-Al_2O_3 coating begin to be lower than that of Ni/GO coating. The phenomenon is more remarkable at the ratio of 1:10 and the corresponding wear rate is about 25×10^{-5} mm^3/Nm, which is also lower than that of Ni/Al_2O_3 coating reported in ref. [37]. Although, statistics are insufficient due to limited samples, with an optimum concentration of GO in the coatings, lower friction coefficient and wear rate can be achieved. Overall, the coefficients reduced with the decreasing ratio of GO in GO-Al_2O_3. Similar results was also reported when embedding GO in the epoxy [35] and copper [29] matrixes.

Fig. 12 gives the wear tracks for Ni/GO-Al_2O_3 composite coatings and pure Ni coating. In Fig. 12a, predominant wear mechanism is adhesive wear when the mass ratio of GO is high. As the ratio of GO reducing, the evidence of abrasive wear behavior is apparent on the wear track and less abrasive grooves along the sliding direction can be found (See Fig. 12b). When the mass ratio reaches to 1:10, the width of wear track decreases remarkably and the track morphology is relatively smooth and shallow with less evidence of grooves. While for pure Ni coating, plastic deformation was observed on the fringe of the sliding surface (Fig. 12e).

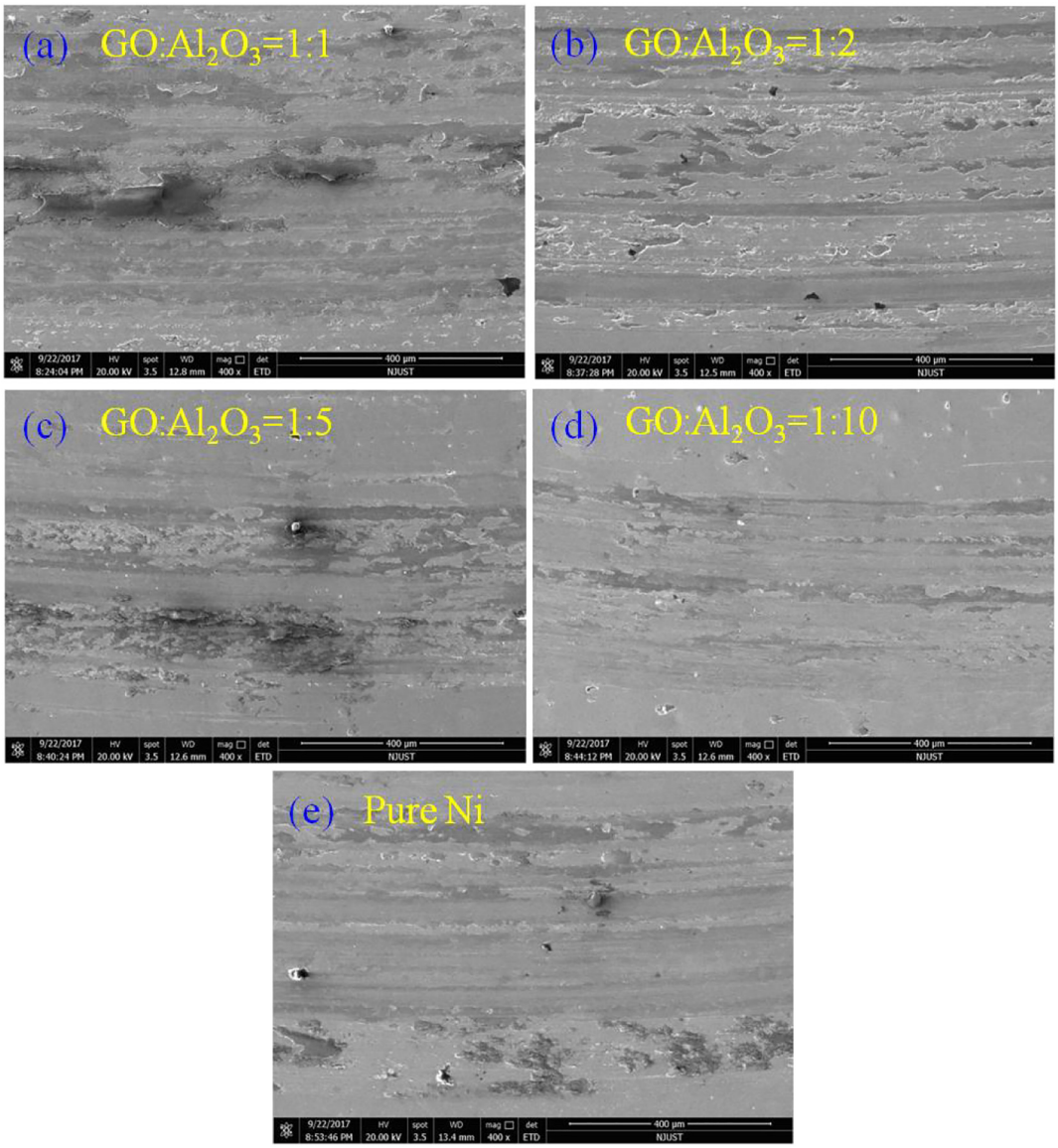

Fig. 12. SEM morphologies analyses of wear tracks.

It seems that the Ni/GO-Al_2O_3 composite coatings with lower ratio of GO and higher ratio of Al_2O_3 present better tribological performances. As mentioned in ref. [38], the higher concentration of GO in the water cannot help reduce friction due to an increased abrasive effect. Meanwhile, at high concentration, the agglomerated GO particles physically form the obstacles between the sliding surfaces while intercepting the interfacial sliding [39]. Consequently, there is a high resistance to shear, and that increases the friction and wear. Besides GO, due to the hard nature of the Al_2O_3, particles in the metal matrix can act as a bearing phase and share most of the load [8,40]. As can be seen in Fig. 11, the wear resistance and hardness of the coatings are related to each other as well as to the particle content. The higher content of Al_2O_3 dispersing in coatings, or at least delay the movement of dislocations in the nickel and thus inhibit the plastic deformation, which result in an increase in the hardness and in an improvement of the wear behavior of the coatings [41].

4. Conclusions

To improve the wear resistance, nickel matrix composite coatings incorporated with GO and GO-Al_2O_3 particles were successfully deposited on copper substrates through electro-deposition. The tribological performances of the composite coatings as well as pure Ni were evaluated under dry sliding condition. It was found that, Ni/GO composite coating exhibits obviously wear resistance and the wear rate reduced by 20.9% compared to pure Ni coating. While for Ni/GO-Al_2O_3 coatings, the lower friction and wear properties were confirmed when depositing GO-Al_2O_3 powder with lower mass ratio of GO. The superior tribological properties of the Ni/GO-Al_2O_3 coatings were attributed to the synergistic effects of GO and Al_2O_3. The experimental results show that the Ni/GO-Al_2O_3 coating with optimized composition has a great potential to be used for wear resistant components.

Acknowledgements

The authors are grateful for the support provided by the Fundamental Research Funds for the Central Universities (No. NE2017104).

References

[1] B.S. Xu, Development of surface engineering in China, Surf. Eng. 26 (2013) 123–125.

[2] M. Stroumbouli, P. Gyftou, E.A. Pavlatou, N. Spyrellis, Codeposition of ultrafine WC particles in Ni matrix composite electrocoatings, Surf. Coat. Technol. 195 (2005) 325–332.
[3] H. Ferkel, B. Müller, W. Riehemann, Electrodeposition of particle-strengthened nickel films, Mater. Sci. Eng. A 234–236 (1997) 474–476.
[4] B.R. Tian, Y.F. Cheng, Electrolytic deposition of Ni–Co–Al2O3 composite coating on pipe steel for corrosion/erosion resistance in oil sand slurry, Electrochim. Acta 53 (2007) 511–517.
[5] B. Szczygieł, M. Kołodziej, Composite Ni/Al_2O_3 coatings and their corrosion resistance, Electrochim. Acta 50 (2005) 4188–4195.
[6] Q. Feng, T. Li, H. Teng, X. Zhang, Y. Zhang, C. Liu, et al., Investigation on the corrosion and oxidation resistance of Ni–Al_2O_3 nano-composite coatings prepared by sediment co-deposition, Surf. Coat. Technol. 202 (2008) 4137–4144.
[7] E. Pompei, L. Magagnin, N. Lecis, P.L. Cavallotti, Electrodeposition of nickel–BN composite coatings, Electrochim. Acta 54 (2009) 2571–2574.
[8] A. Tang, M. Wang, W. Huang, X. Wang, Composition design of Ni–nano-Al_2O_3–PTFE coatings and their tribological characteristics, Surf. Coat. Technol. 282 (2015) 121–128.
[9] W. Huang, Y. Zhao, X. Wang, Preparing a high-particle-content Ni/diamond composite coating with strong abrasive ability, Surf. Coat. Technol. 235 (2013) 489–494.
[10] N.K. Shrestha, D.B. Hamal, T. Saji, Composite plating of Ni-P-Al_2O_3 in two steps and its anti-wear performance, Surf. Coat. Technol. 183 (2004) 247–253.
[11] A. Mohamed Mahmoud Ibrahim, X. Shi, W. Zhai, J. Yao, Z. Xu, L. Cheng, et al., Tribological behavior of NiAl–1.5 wt% graphene composite under different velocities, Tribol. Trans. 57 (2014) 1044–1050.
[12] S.J. Hall, T. Murphy, The effect of graphene content and sliding speed on the wear mechanism of nickel-graphene nanocomposites, Appl. Surf. Sci. 359 (2015) 340–348.
[13] J. Chen, J. Li, D. Xiong, Y. He, Y. Ji, Y. Qin, Preparation and tribological behavior of Ni-graphene composite coating under room temperature, Appl. Surf. Sci. 361 (2016) 49–56.
[14] C. Min, C. Shen, M. Zeng, P. Nie, H.-J. Song, S. Li, Influence of graphene oxide as filler on tribological behaviors of polyimide/graphene oxide nanocomposites under seawater lubrication, Monatsh. Chem. Chem. Mon. 148 (2017) 1301–1309.
[15] C. Qiu, D. Liu, K. Jin, L. Fang, T. Sha, Corrosion resistance and micro-tribological properties of nickel hydroxide-graphene oxide composite coating, Diam. Relat. Mater. 76 (2017) 150–156.
[16] C. Liu, F. Su, J. Liang, Producing cobalt–graphene composite coating by pulse electrodeposition with excellent wear and corrosion resistance, Appl. Surf. Sci. 351 (2015) 889–896.
[17] H. Algul, M. Tokur, S. Ozcan, M. Uysal, T. Cetinkaya, H. Akbulut, et al., The effect of graphene content and sliding speed on the wear mechanism of nickel–graphene nanocomposites, Appl. Surf. Sci. 359 (2015) 340–348.
[18] Z. Xue, W. Lei, Y. Wang, H. Qian, Q. Li, Effect of pulse duty cycle on mechanical properties and microstructure of nickel-graphene composite coating produced by pulse electrodeposition under supercritical carbon dioxide, Surf. Coat. Technol. 325 (2017) 417–428.
[19] H. Wu, F. Liu, W. Gong, F. Ye, L. Hao, J. Jiang, et al., Preparation of Ni–P–GO composite coatings and its mechanical properties, Surf. Coat. Technol. 272 (2015) 25–32.
[20] J. Jiang, H. Chen, L. Zhu, W. Qian, S. Han, H. Lin, et al., Effect of heat treatment on structures and mechanical properties of electroless Ni-P-GO composite coatings, RSC Adv. 6 (2016) 109001–109008.
[21] J. Chen, B. Yao, C. Li, G. Shi, An improved hummers method for eco-friendly synthesis of graphene oxide, Carbon 64 (2013) 225–229.
[22] Y. Zhu, S. Murali, W. Cai, X. Li, J.W. Suk, J.R. Potts, et al., Graphene and graphene oxide: synthesis, properties, and applications, Adv. Mater. 22 (2010) 3906–3924.
[23] A. Wang, X. Li, Y. Zhao, W. Wu, J. Chen, H. Meng, Preparation and characterizations of Cu_2O/reduced graphene oxide nanocomposites with high photo-catalytic performances, Powder Technol. 261 (2014) 42–48.
[24] X.J. Wang, B. Dong, M.K. Lei, Infrared absorption spectra of Er^{3+}-doped Al_2O_3 nanopowders by the sol-gel method, J. Sol-Gel Sci. Technol. 39 (2006) 307–311.
[25] Y. Zeng, X. Pei, S. Yang, H. Qin, H. Cai, S. Hu, et al., Graphene oxide/hydroxyapatite composite coatings fabricated by electrochemical deposition, Surf. Coat. Technol. 286 (2016) 72–79.
[26] H. Song, Z. Wang, J. Yang, Tribological properties of graphene oxide and carbon spheres as lubricating additives, Appl. Phys. A Mater. Sci. Process. 122 (2016).
[27] B. Lee, M.Y. Koo, S.H. Jin, K.T. Kim, S.H. Hong, B. Lee, et al., Simultaneous strengthening and toughening of reduced graphene oxide/alumina composites fabricated by molecular-level mixing process, Carbon 78 (2014) 212–219.
[28] I. Garciaa, J. Fransaer, J.P. Celis, Electrodeposition and sliding wear resistance of nickel composite coatings containing micron and submicron SiC particles, Surf. Coat. Technol. 148 (2001) 171–178.
[29] H.S. Maharana, P.K. Rai, A. Basu, Surface-mechanical and electrical properties of pulse electrodeposited Cu–graphene oxide composite coating for electrical contacts, J. Mater. Sci. 52 (2017) 1089–1105.
[30] S. Alirezaei, S.M. Monirvaghefi, M. Salehi, A. Saatchi, Wear behavior of Ni-P and Ni-P-Al_2O_3 electroless coatings, Wear 262 (2007) 978–985.
[31] L. Zhang, Y. He, S. Feng, L. Zhang, L. Zhang, Z. Jiao, et al., Preparation and tribological properties of novel boehmite/graphene oxide nano-hybrid, Ceram. Int. 42 (2016) 6178–6186.
[32] N. Nemati, M. Emamy, S. Yau, J.K. Kim, D.E. Kim, High temperature friction and wear properties of graphene oxide/polytetrafluoroethylene composite coatings deposited on stainless steel, RSC Adv. 6 (2016) 5977–5987.
[33] D. Berman, A. Erdemir, A.V. Sumant, Graphene: a new emerging lubricant, Mater. Today 17 (2014) 31–42.
[34] H. Liang, Y. Bu, J. Zhang, Z. Cao, A. Liang, Graphene oxide film as solid lubricant, ACS Appl. Mater. Interfaces 5 (2013) 6369–6375.
[35] X.-J. Shen, X.-Q. Pei, S.-Y. Fu, K. Friedrich, Significantly modified tribological performance of epoxy nanocomposites at very low graphene oxide content, Polymer 54 (2013) 1234–1242.
[36] L.B. Tong, J.B. Zhang, C. Xu, X. Wang, S.Y. Song, Z.H. Jiang, et al., Enhanced corrosion and wear resistances by graphene oxide coating on the surface of Mg-Zn-Ca alloy, Carbon 109 (2016) 340–351.
[37] L. Chen, L. Wang, Z. Zeng, J. Zhang, Effect of surfactant on the electrodeposition and wear resistance of Ni–Al_2O_3 composite coatings, Mater. Sci. Eng. A 434 (2006) 319–325.
[38] O. Elomaa, V.K. Singh, A. Iyer, T.J. Hakala, J. Koskinen, Graphene oxide in water lubrication on diamond-like carbon vs. stainless steel high-load contacts, Diam. Relat. Mater. 52 (2015) 43–48.
[39] B. Gupta, N. Kumar, K. Panda, S. Dash, A.K. Tyagi, Energy efficient reduced graphene oxide additives: mechanism of effective lubrication and antiwear properties, Sci. Rep. 6 (2016) 18372.
[40] Z.J. Huang, D.S. Xiong, MoS_2 coated with Al_2O_3 for Ni–MoS_2/Al_2O_3 composite coatings by pulse electrodeposition, Surf. Coat. Technol. 202 (2008) 3208–3214.
[41] E. García-Lecina, I. García-Urrutia, J.A. Díez, J. Morgiel, P. Indyka, A comparative study of the effect of mechanical and ultrasound agitation on the properties of electrodeposited Ni/Al_2O_3 nanocomposite coatings, Surf. Coat. Technol. 206 (2012) 2998–3005.